System Design of a Tethered Robotic Explorer (TReX) for 3D Mapping of Steep Terrain and Harsh Environments

Patrick McGarey, François Pomerleau, and Timothy D. Barfoot

Abstract The use of a tether in mobile robotics provides a method to safely explore steep terrain and harsh environments considered too dangerous for humans and beyond the capability of standard ground rovers. However, there are significant challenges yet to be addressed concerning mobility while under tension, autonomous tether management, and the methods by which an environment is assessed. As an incremental step towards solving these problems, this paper outlines the design and testing of a center-pivoting tether management payload enabling a four-wheeled rover to access and map steep terrain. The chosen design permits a tether to attach and rotate passively near the rover's center-of-mass in the direction of applied tension. Prior design approaches in tethered climbing robotics are presented for comparison. Tests of our integrated payload and rover, Tethered Robotic Explorer (TReX), show full rotational freedom while under tension on steep terrain, and basic autonomy during flat-ground tether management. Extensions for steep-terrain tether management are also discussed. Lastly, a planar lidar fixed to a tether spool is used to demonstrate a 3D mapping capability during a tethered traverse. Using visual odometry to construct local point-cloud maps over short distances, a globally-aligned 3D map is reconstructed using a variant of the Iterative Closest Point (ICP) algorithm.

1 Introduction

Robotic planetary and terrestrial exploration has historically been risk-averse, favoring benign terrain in order to reduce the likelihood of mission failure [12]. Even state-of-the-art rovers deployed on Mars are not suited to access steep terrain directly, and instead rely on remote observation [7]. As we push towards developing

Patrick McGarey, François Pomerleau, Timothy D. Barfoot, University of Toronto Institute for Aerospace Studies, Toronto, Canada, e-mail: patrick.mcgarey@robotics.utias.utoronto.ca, francois.pomerleau@robotics.utias.utoronto.ca , tim.barfoot@utoronto.ca

autonomous systems for harsh terrain, tethering (i.e., attachment of supportive electromechanical cable or climbing rope between a robot and an anchor point) will not only be necessary for safety and mobility, but also a benefit to robots requiring both assistive power and robust communication throughout challenging traverses.

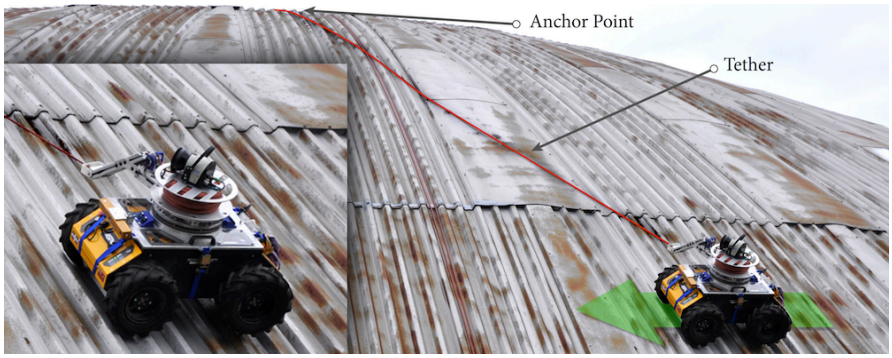

Fig. 1 Our Tethered Robotic Explorer (TReX) traverses the exterior of a dome structure, showing lateral motion (green arrow) under tension.

Geologic exploration of steep terrain, safety inspection of walls and dams, and disaster response in resource- and communication-limited environments, are typical applications appropriate for tethered robots. Detailed point-cloud maps constructed from lidar data enable geologists to model vertical stratigraphy at high resolution [9]. Robots inspecting walls and dams allow for repeated observations of targeted areas as a means to evaluate temporal changes and reduce risk to humans [11]. Deploying robots to assist in disaster response may require that wired communication and external power sources are provided due to extended operation in resource-limited environments. The use of a tether offers a solution to power and communication requirements. However, tether management still presents a significant challenge to robots operating in dangerous conditions [8].

While prior systems have addressed these challenges with some success, it is the opinion of the authors that a lack of autonomy has attenuated continued progress in tethered mobile robotics. In order to make advancements in autonomous mobility, tether management, and environmental mapping, we have developed a new research platform, Tethered Robotic Explorer (TReX).

This paper is organized as follows. Section 2 evaluates prior tethered climbing rovers, Section 3 details the system design of TReX, Section 4 presents experimental results, Section 5 provides lessons learned, and Section 6 offers conclusions.

2 Related Work

The archetype of tethered climbing robots was Dante II (Figure 2a), an eight-legged walking rover used to traverse the interior craters of volcanoes [15]. Dante II successfully repelled down extreme slopes and demonstrated the challenges/limitations of tethered mobility; during an ascent of a crater, Dante II was critically damaged from a fall while rotating outside the direction of applied tension.

Teamed Robots for Exploration and Science on Steep Areas (TRESSA) (Figure 2b) was the first modular system allowing an attached flat-ground rover to access vertical terrain [14]. The off-board managed dual-tether configuration provided easy integration with different rovers and allowed some lateral motion on steep terrain. However, multiple tethers implied an increased difficulty navigating around obstacles, tether abrasion, and reduced range due to dragging (tethers were not spooled on the robot).

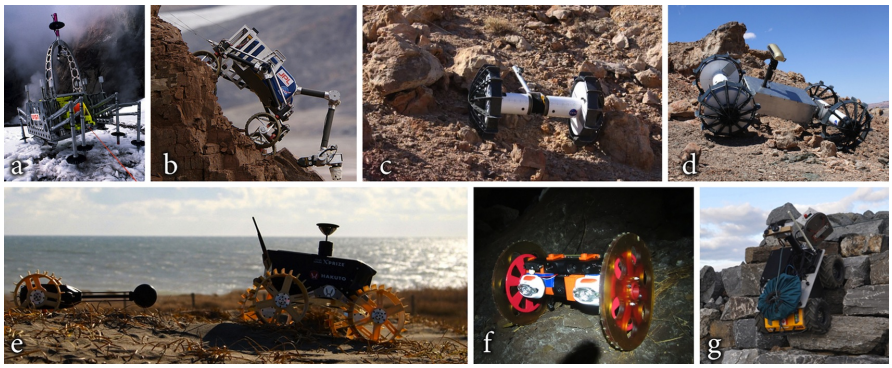

Fig. 2 Past and present tethered climbing rovers: *a*) Dante II [2], *b*) TRESSA [5], *c*) Axel II and *d*) DuAxel [7], *e*) Tetris and Moonraker [3], *f*) VolcanoBot II (JPL/CalTech), and *g*) vScout [13]

The most capable tethered climbing robot to date has been Axel II (Figure 2c), a two-wheeled rover with an actuated tether caster arm [7]. Multiple Axel II rovers could be linked by a docking station to operate as either a four-wheeled rover (i.e., DuAxel), or as a redundant base station and climbing rover (Figure 2d). Axel II's innovative configuration has been adapted by the Moonraker and Tetris robots [1] (Figure 2e), and VolcanoBot [2] (Figure 2f).

The vScout prototype (shown in Figure 2g) consisted of a winch payload mounted to a Clearpath Husky A200 rover [13]. The prototype was a precursor to TReX. While the tether was not actively managed on board, vScout successfully demonstrated the maneuverability of a 50 kg commercial rover on steep slopes.

Prior tethered climbing robots have shown minimal vehicle rotational range centered around the direction of applied tension on steep slopes, implying both an in-

[1] Moonraker and Tetris were developed by Team Hakutu from Tohoku University

[2] VolcanoBot II is a small rover used for mapping volcanic vents, JPL/Caltech

creased risk of entanglement with obstacles, and limitations on drivable paths. The design of TReX considered both attributes and limitations of prior designs.

3 System Design

3.1 Tethered Robotic Explorer (TReX)

In order for a tethered rover to rotate continuously under tension, a tether is connected to a freely rotating joint. When taut, the tether's tensional force is aligned with a virtual line intersecting the vehicle's center-of-mass. The on-board managed tether is wound around an actuated spool, which is mounted to a rotational joint in the center of a skid-steered Clearpath Husky A200 rover. A cut view of the TReX CAD model shown in Figure 3 illustrates the mounting configuration of the spool on a rotating tether arm, which mechanically links to the rover using a slew bearing. The three rotating elements (rover, tether arm, and spool) are outlined in colored

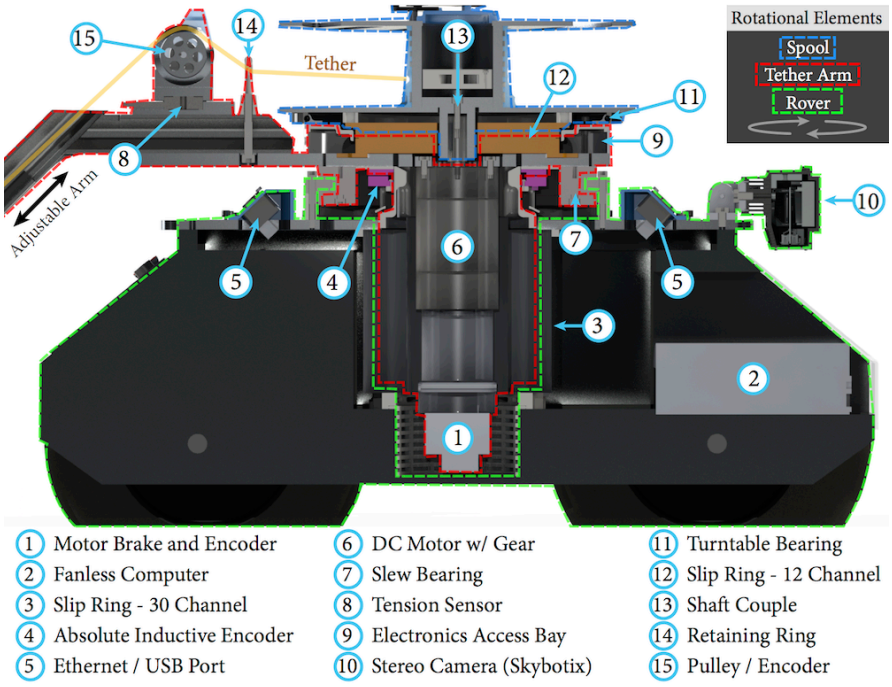

Fig. 3 Annotated CAD model (cut view). The three rotating elements include the rover (green), tether arm (red), and spool (blue). The tether spool is actuated only when motorized. Major internal components are labeled. Note that the tether arm, lidar, and rover wheels have been cropped.

dashed lines. The spool, which rests on a separate turntable bearing above the tether arm, can only rotate when actuated by a motor. The motor, which is suspended in the 10 cm cavity of a rotary slip ring, is fixed to the tether arm, while its shaft is coupled to the spool. To reduce torque on the rover, a manually adjustable angled arm allows for load balancing with the vehicle's center-of-mass. The design permits the rover to rotate freely regardless of applied tension, provided there is sufficient wheel traction.

Sensor interfacing requires careful consideration of the design's rotational degrees of freedom. In order to produce three-dimensional (3D) point-clouds with a planar scanning lidar, the sensor is mounted on the rotating tether spool. This configuration allows for a single actuator (not including vehicle wheels) to be used in tether management and 3D mapping. Since the rotation of the lidar is coupled to a tether spool, 3D scanning is only possible when the vehicle is moving and the tether is actively being managed. Providing power to and receiving data from the lidar requires two Ethernet-enabled slip rings that bridge three separate rotating elements (the electronic configuration used for the lidar is adaptable to other types of Ethernet-enabled sensors if desired). A junction within the spool cylinder allows an optional electromechanical tether to be connected. When connected, TReX can leverage external power sources, continuous battery charging, and Power-over-Ethernet (PoE) communication. Sensors and electrical interfaces housed in the tether arm and spool are connected to the rover through the lower 30-channel slip ring. The motor's power is supplied through several high-current channels in the same 30-channel slip ring. A stereo camera mounted on the front of the vehicle is used for visual odometry, terrain imaging, and live display for tele-operation. The on-board fanless computer serves in data collection, processing, and communication with a base station.

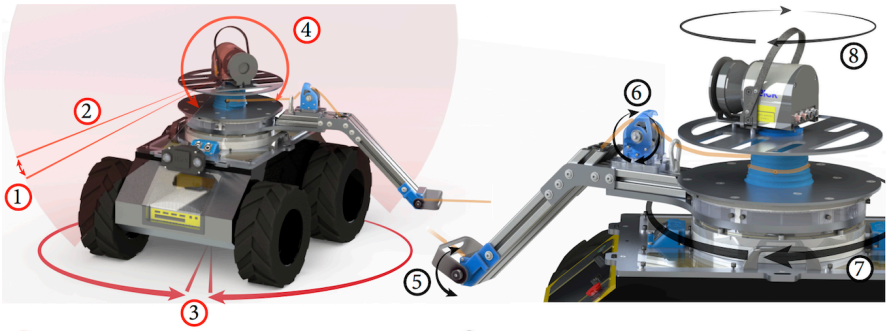

1. Elevation Scan Spacing : 0.5°
2. Effective Range: 0.5 m to 50 m
3. Worst-Case Azimuth Scan Spacing: 1.7°
4. Planar Field-of-View: 270°
5. Tether Pitch Potentiometer: [-90°, 90°]
6. Tether Length Encoder: 100 ppr Quadrature
7. Tether Yaw Encoder: 16-bit Absolute Positioning
8. Spool Encoder: 9600 ppr Quadrature

Fig. 4 *Left*: 3D Mapping specifications. The lidar plane is shown by an opaque red disk. *Right*: Tether orientation and sensor specifications. The locations of measurement for pitch, length, and yaw are indicated. The spool encoder provides rotational measurements for the lidar.

TReX's ability to map an environment using 3D point-clouds and to accurately measure tether orientation are illustrated in Figure 4. In terms of 3D mapping, the *left* illustration shows the lidar scan plane, and provides specifications on the range and rotational scan spacing. The *right* image shows how tether orientation is measured. Tether yaw (i.e., bearing to current anchor point) is measured at the rotating joint between the tether arm and rover. Tether pitch is measured using the c-shaped extension mounted on the angled arm. Tether length is measured by a combined pulley-and-force-plate assembly mounted on the tether arm. The spool encoder is used to measure lidar rotation with respect to the tether arm. Given the maximum spool motor speed (≈ 0.23 rps) and the scanning frequency of the lidar (≈ 50 Hz), the worst-case azimuth scan spacing is 1.7° (0.029 rad) when the vehicle is under tension.

Lastly, Figure 5 provides as-built system specifications and an image of the final build. The payload was tailored for the Clearpath Husky A200 rover due to its successful implementation in the vScout prototype.

Final As-Built Specifications

Mass	92 Kg (tether included)
Dimension	1.06 x 0.67 x 0.76 m
Power	24VDC, 120VAC
Platform	Clearpath Husky A200
Actuator	MMP 170 Nm Torque
Camera	Skybotix VI-Sensor
Lidar	Sick LMS151
Computer	Logic Nuvo-3100VTC
DAQ	Lab Jack T7
Tether	50 m to 100 m

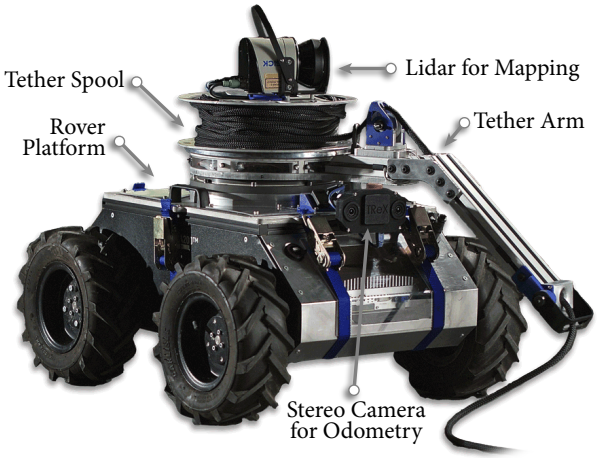

Fig. 5 *Left*: Final system specifications. *Right*: TReX with major systems labeled. We note that the stereo camera may be occluded by the tether arm during a traverse. However, the pivoting tether arm allows for reorientation of the rover and camera while under tension.

3.2 Comparison To Prior Systems

Figure 6 presents an illustrated comparison between past tethered climbing rovers and TReX. The comparison allows for a qualitative evaluation of tethered maneuverability on steep terrain, and demonstrates the benefit of added rotational freedom while under tension.

1) Rotational Freedom: Prior tethered climbing robots have lacked the ability to turn significantly outside the direction of applied tension on steep terrain. TReX

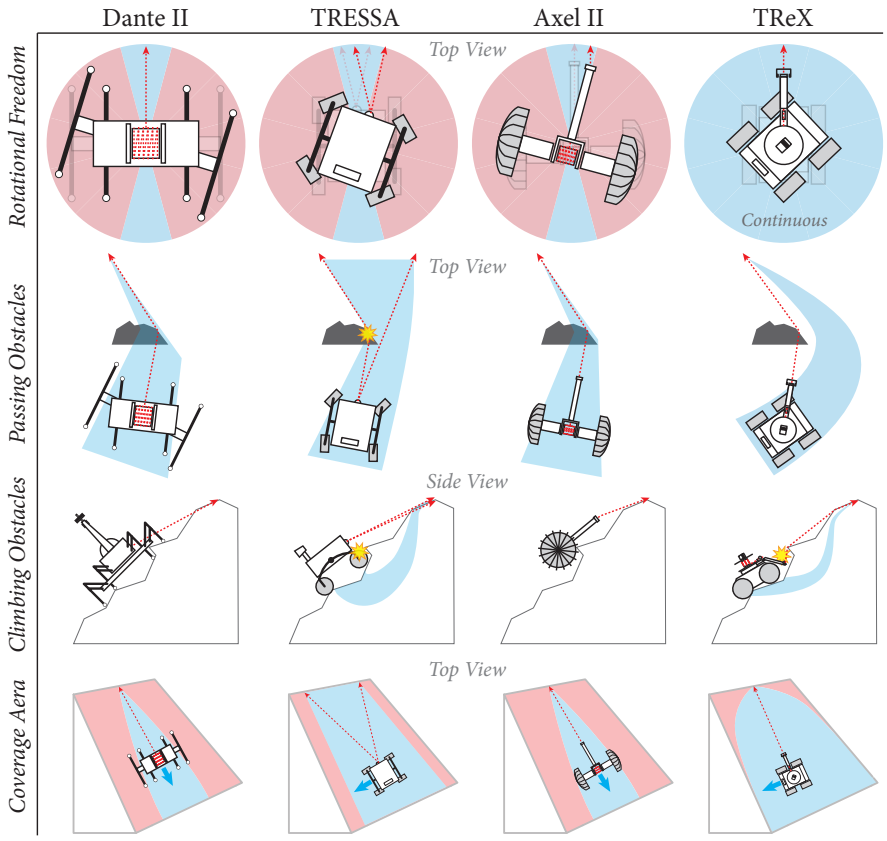

Fig. 6 Maneuverability comparison of Dante II, TRESSA, Axel II, and TReX (figure not drawn to scale). Each row represents attributes of tethered mobility: *Rotational Freedom*, *Passing Obstacles*, *Climbing Obstacles*, and *Coverage Area (single traverse)*. Each column corresponds to a different vehicle. View orientations are given by row (e.g., top and side). All vehicles with the exception of TRESSA manage tether on board. Tether is indicated by dashed red lines, while interactions with obstacles are shown with yellow stars. The light blue and red colors represent feasible and infeasible rotations/paths, respectively. Small blue arrows indicate vehicle heading.

allows continuous rotation about a center-pivot point, which enables horizontal motion while under tension, provided there is sufficient wheel traction.

2) Passing Obstacles: Obstacles may serve as additional anchor points for tethered rovers. Without the ability to rotate outside the direction of applied tension, obstacles serving as anchor points must be approached directly. Dante II and Axel II were designed for rough terrain and may traverse mid-sized obstacles. While TRESSA has some ability to drive laterally, its dependence on two discrete off-board winches implies higher tether abrasion due to dragging cables. TReX has the unique ability to rotate perpendicular to any anchor point, resulting in an improved method for passing obstacles.

3) Climbing Obstacles: Harsh, obstacle-ridden slopes may be difficult, if not impossible, for flat ground vehicles to traverse due to smaller wheel radii and terrain clearance issues. While TReX may encounter insurmountable obstacles along a traverse, its rotational freedom may allow for an alternate path to be taken if feasible. Although TRESSA can perform a similar maneuver, its lateral range is limited by the baseline configuration of top-mounted anchor winches. Furthermore, tether abrasion or entanglement become a concern due to off-board management.

4) Coverage Area: The effective coverage area of a single traverse is directly related to a rover's ability to translate laterally on steep slopes. Outside of significantly steep terrain, causing a reduction of traction and horizontal mobility, TReX provides increased access to steep areas in comparison to prior rovers. We note that TRESSA allows some lateral motion in the absence of wheel traction at the cost of tether control complexity.

4 Experimental Results

4.1 Rover Maneuverability

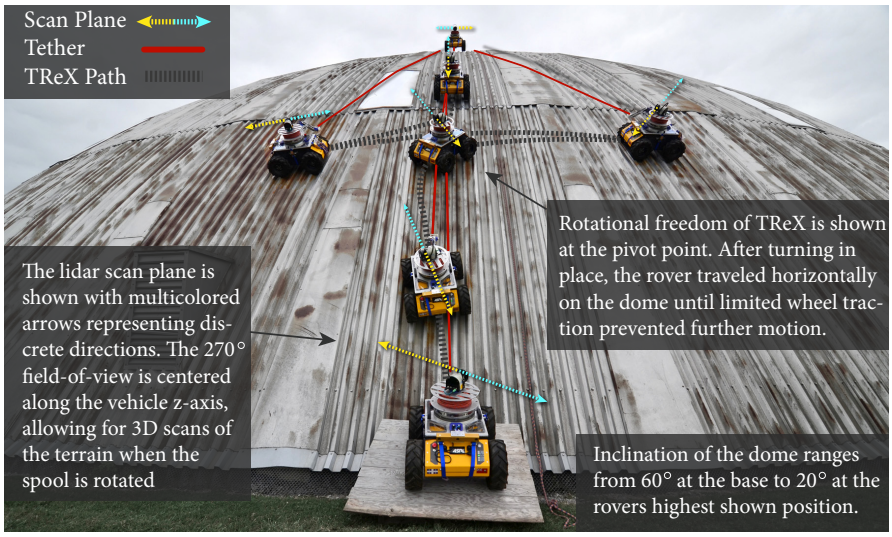

Fig. 7 TReX was manually piloted in a maneuverability test on a 50 m dome while under tension.

An initial evaluation of rover maneuverability was performed on the exterior of a 50-m-diameter dome (MarsDome) located at the University of Toronto Institute for Aerospace Studies (UTIAS). A composite time-lapse image of this test is shown in Figure 7. TReX was manually operated over varying slopes, demonstrating tether-

assisted mobility and rotational freedom under tension. The overlaid yellow and blue arrows represent discrete sides of the lidar scan plane. The coverage area (i.e., the combined point-cloud) depends on the rotation of the spool with respect to the world.

4.2 Tether Management

Autonomy in tether management presents a significant barrier to mobility on steep slopes, especially in the presence of obstacles. To the best knowledge of the authors, no tethered climbing rover has fully implemented autonomous tether management in field experimentation. Tether management was first considered for mobile robots in the mechanical design of Dante II [6]. The developers of TRESSA and Axel II have proposed a method for tether management based on inclination, mass, and tether orientation [14, 1]. However, this has yet to be demonstrated in field testing.

Provided that tension is measured, tether management on flat ground relies on the selection of a static reference tension to maintain. On steep terrain, the influence of gravity on the rover's mass makes the selection of an appropriate reference tension nontrivial. An evaluation of tension-based tether management with the TReX platform is discussed in the following sections.

4.2.1 Tether Management on Flat Ground

Tether management on flat ground utilizes a tension-based controller, which is not reliant on feed-forward input from the rover. Figure 8 illustrates the closed-loop spool velocity controller. The overall goal is to maintain an adequate tension while preserving maneuverability.

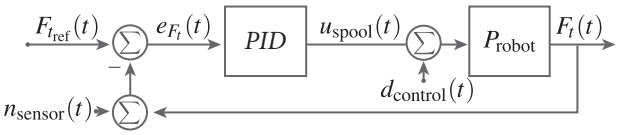

Fig. 8 Closed-loop feedback controller. The error between $F_{t_{\text{ref}}}(t)$ and $F_t(t)$ (reference and measured force) is $e_{F_t}(t)$. A gain, $K(t)$, is computed using a PID. The resulting spool control input, $u_{\text{spool}}(t)$, is the maximum spool velocity scaled by $K(t)$. The robot plant is P_{robot}. The inputs, $n_{\text{sensor}}(t)$ and $d_{\text{control}}(t)$, correspond to sensor noise and control disturbances, respectively.

As a basic test of the flat-ground tension-based controller, TReX was driven in the presence of a Vicon motion-capture system. The position of the rover, tether arm, and anchor point were recorded during two traverses. Figure 9 provides a colorized representation of tether tension and orientation with respect to the known rover position and anchor point. An accompanying time-lapse image of the exper-

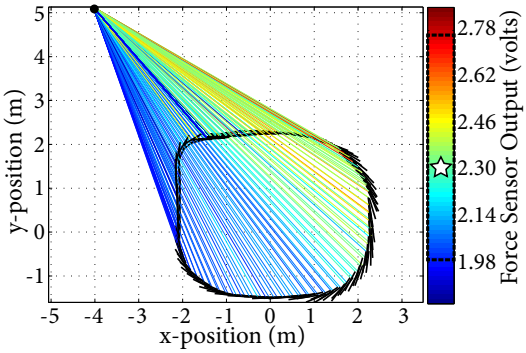

Fig. 9 Tension sensor output is illustrated by colorized tether vectors corresponding to volts. Black lines along the path represent vehicle headings. The dashed box on the color legend corresponds to the range of voltages sensed, while the star indicates the desired reference tension.

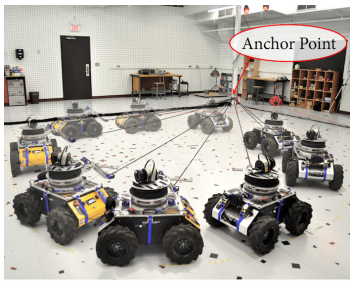

Fig. 10 A time-lapse of the Vicon test shows TReX performing tension-based tether management. Throughout two traverses, the tether was taut with minimal sag.

iment is shown in Figure 10. The range of sensed volts indicated by a dashed box in the figure shows that extremes in measurement were avoided (i.e., the tether remained generally taut throughout, and at no point did it touch the ground or prevent the rover from driving its path). Volts are shown in place of kilograms force for this figure due to inaccuracies in calibration/measurement, which are discussed in the proceeding section. Further development of the controller will be necessary in order to compensate for the disparity between reeling conditions (i.e., there is currently a distinct trend in tension error when traversing to or away from the anchor point).

4.2.2 Extensions Towards Steep Terrain

Steep-terrain tether management requires an understanding of sensor performance at varying inclinations. The force sensor used in the design is provided with a factory-calibrated linear output (given in terms of volts per unit force). Unfortunately, frictional elements within the angled-arm design cause a hysteresis-influenced sensor response, where loading and unloading conditions imply different output measurements at similar inclinations. We attempted to characterize hysteresis using an angled-plane test. During the test, TReX was fixed to an anchor point and the plane angle, θ, was cycled between 0° and 90°. Three tests were performed where the tether pitch was varied with respect to the plane as shown in Figure 11.

The result of three angled-plane tests with variations in tether pitch are shown in Figure 12. Only test 1 shows a full cycle of the plane θ between 0° and 90°. In tests 2 and 3, the rover's rear tires left the plane due to applied torque on the tether arm at steep inclinations as noted in Figure 12. Fortunately, the tests were still useful in determining an overall trend in sensor response due to variations in tether pitch and plane inclination.

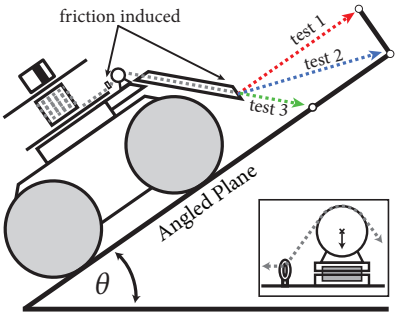

Fig. 11 Angled-plane test (illustrated). TReX was fixed statically on the plane, while variations of tether pitch and plane inclination, θ, were tested. The plane θ was cycled between 0° and 90°. The colors correspond to different tests in Figure 12. Force sensor placement is shown by a gray box in the inset illustration.

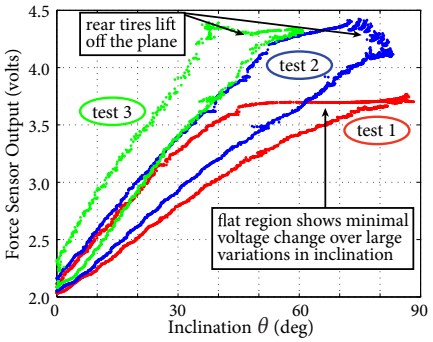

Fig. 12 Sensor hysteresis over three lifting cycles with varied tether pitch. The lower portion of the wing-shaped pattern represents loading, while the upper is unloading. The plot indicates that tension was lost due to friction. Test 1 displayed the most loss, suggesting that friction inducing parts should be replaced in the arm.

In the first test, tether pitch was constrained parallel to the plane of inclination. While unloading, friction between the arm and tether resulted in an unchanged sensor output until stiction was overcome near 45°. During a second test, the tether pitch was set to 25°. The voltage output in test 2 generally increased in comparison to test 1, suggesting that friction had been reduced by increasing tether pitch; the increased pitch minimized the contact surface and bending moment of the tether on the mechanical fairlead. In test 3, the fairlead was completely removed to evaluate its impact on sensor measurement. Tether pitch was constrained to 45°, matching the tilt of the angled arm. Removing the fairlead caused the entire sensor output to increase substantially from what was observed in the first two tests. However, the continued disparity between loading and unloading conditions suggested that friction was still a factor elsewhere in the tether arm design. The most likely source was the steel retaining ring located before the pulley. Unfortunately, the ring was critical to maintaining a balanced load over the pulley and force sensor, and could not be removed to test its frictional impact.

Problems in the tether arm design made a repeatable characterization of the force sensor impossible. Therefore, moving towards tension-based tether management on steep terrain will require modifications to the arm design as proposed in Section 5.

4.3 3D Point Cloud Mapping

The collection of a single 3D point-cloud is triggered after every 180° rotation of a lidar with respect to the world frame. Visual odometry is used to locally provide a motion estimate of the lidar during this time. Once a series of point-clouds have been

recorded, a global representation is generated using an efficient variant of Iterative Closest Point (ICP) relying on libpointmatcher [10].

As an initial test of this 3D mapping functionality, TReX was anchored and manually piloted through an indoor environment with obstacles to produce a fused 3D point-cloud map. Figure 13, provides multiple views of the reconstructed environment, as well as a time-lapse image of the test. Odometry was provided by a Skybotix VI-Sensor stereo camera, which outputs a pair of calibrated images to an open-source library, Fast Odometry from VISion (FOVIS) [3]. The library functions by detecting similar features in stereo images as a means to compute a velocity and output a camera pose [4].

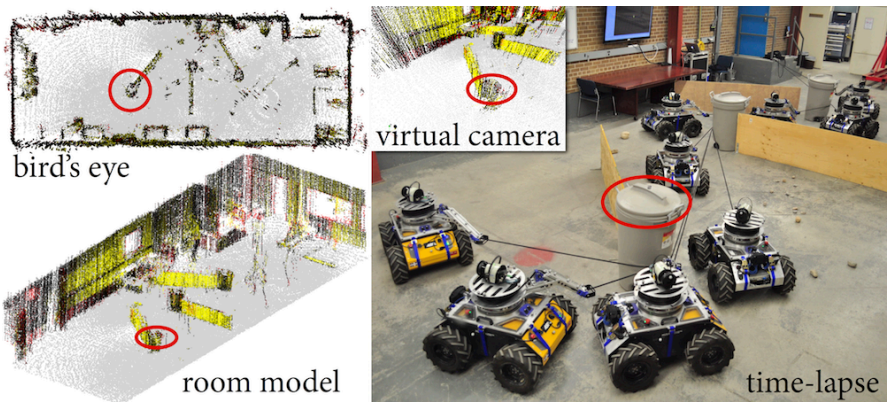

Fig. 13 Combined point-cloud of an indoor workshop with a time-lapse image of the test. All maps are point representations with correlated intensity. Obstacles were placed in the room to prevent TReX from performing a full scan before driving. The rover was driven around three weighted plastic bins, filling in portions of the map along the way. Red circles correspond to the same bin.

5 Lessons Learned

With respect to the experimental results previously discussed, engineering lessons learned in the design and initial testing of TReX are summarized by category below.

Platform Maneuverability: When rotation is constrained, linear motion is limited to the direction of tension. For Dante II, TRESSA, and Axel II, this means that vehicle motion on steep terrain is generally linear, where vehicle velocities directly correlate to tether velocities. For TReX, full range of motion implies that tether velocity is a factor of the current vehicle pose, commanded linear/angular velocities, and position of the anchor point. Excessive inclinations denote higher wheel slippage, resulting in a need for tether-assisted mobility (e.g., commanded vehicle motion is converted into tether actions). For this to occur, we must localize the robot on steep terrain and sense when and where new anchor points have been added.

[3] package available: https://github.com/srv/fovis

Tether Management: Tension-based tether management on steep terrain was not demonstrated due to the accumulation of friction in the tether arm. The friction implied a significant variation in sensor output during repeated tests. As such, the tether arm requires modification in the form of additional pulley wheels or bearings to replace friction-inducing parts. When greater repeatability is achieved, then a characterization of the force sensor at varying inclinations should allow for a tension-based controller to be tested on moderate slopes. When the wheel traction is sufficiently reduced in steep terrain, the rover will require tether-assisted mobility. A feed-forward tether management controller, where piloted vehicle actions correspond to appropriate tether actions, will be evaluated.

3D Point Cloud Mapping: Point misalignment in the 3D map shown in Figure 13 stems from poor visual odometry calibration as well sensor drift in the spool angle encoder. The first issue is likely related to an inaccurate measurement of the camera pose transformation to the vehicle frame. The sensor drift problem stems from measuring angular position before the gearing on the motor. This means that several hundred rotations will occur before a complete rotation is sensed. The addition of a magnetic hall effect sensor on the spool could help in reducing drift. Finally, the scan spacing of the rotating lidar is dependent on spool velocity with respect to the world frame. The impact of variances in rotating elements generate nonuniform radial densities for points, as the rotational speed of the sensor is dependent on the environment. Accordingly, an in-depth evaluation of the 3D point reconstruction pipeline is necessary.

6 Conclusion

This work describes the system design and initial testing of a new tethered climbing rover. Tethered Robotic Explorer (TReX) allows for 3D mapping in steep terrain and harsh environments, and is intended to be used for cliff exploration, dam safety inspection, and disaster response. Tests of rotational freedom while under tension, tension-based tether management in varied terrain, and 3D mapping capabilities have demonstrated that the center-pivoting TReX offers improved methods for steep terrain navigation in comparison to prior tethered climbing rovers.

References

[1] Abad-Manterola, P.: Axel rover tethered dynamics and motion planning on extreme planetary terrain. Ph.D. thesis, California Institute of Technology (2012)

[2] Bares, J.E., Wettergreen, D.S.: Dante II: Technical description, results, and lessons learned. The International Journal of Robotics Research **18**(7), 621–649 (1999)

[3] Britton, N., Yoshida, K., Walker, J., Nagatani, K., Taylor, G., Dauphin, L.: Lunar micro rover design for exploration through virtual reality tele-operation. In: Field and Service Robotics, pp. 259–272. Springer (2015)
[4] Huang, A.S., Bachrach, A., Henry, P., Krainin, M., Maturana, D., Fox, D., Roy, N.: Visual odometry and mapping for autonomous flight using an RGB-D camera. In: International Symposium on Robotics Research (ISRR), pp. 1–16 (2011)
[5] Huntsberger, T., Stroupe, A., Aghazarian, H., Garrett, M., Younse, P., Powell, M.: Tressa: Teamed robots for exploration and science on steep areas. Journal of Field Robotics **24**(11-12), 1015–1031 (2007)
[6] Krishna, M., Bares, J., Mutschler, E.: Tethering system design for dante ii. In: Robotics and Automation, 1997. Proceedings., 1997 IEEE International Conference on, vol. 2, pp. 1100–1105. IEEE (1997)
[7] Matthews, J.B., Nesnas, I.A.: On the design of the axel and duaxel rovers for extreme terrain exploration. In: Aerospace Conference, 2012 IEEE, pp. 1–10. IEEE (2012)
[8] Nagatani, K., Kiribayashi, S., Okada, Y., Otake, K., Yoshida, K., Tadokoro, S., Nishimura, T., Yoshida, T., Koyanagi, E., Fukushima, M., et al.: Emergency response to the nuclear accident at the Fukushima Daiichi Nuclear Power Plants using mobile rescue robots. Journal of Field Robotics **30**(1), 44–63 (2013)
[9] Osinski, G.R., Barfoot, T.D., Ghafoor, N., Izawa, M., Banerjee, N., Jasiobedzki, P., Tripp, J., Richards, R., Auclair, S., Sapers, H., et al.: Lidar and the mobile scene modeler (msm) as scientific tools for planetary exploration. Planetary and Space Science **58**(4), 691–700 (2010)
[10] Pomerleau, F., Colas, F., Siegwart, R., Magnenat, S.: Comparing ICP Variants on Real-World Data Sets. Autonomous Robots **34**(3), 133–148 (2013)
[11] Ridao, P., Carreras, M., Ribas, D., Garcia, R.: Visual inspection of hydroelectric dams using an autonomous underwater vehicle. Journal of Field Robotics **27**(6), 759–778 (2010)
[12] Schenker, P.S., Elfes, A., Hall, J.L., Huntsberger, T.L., Jones, J.A., Wilcox, B.H., Zimmerman, W.F.: Expanding venue and persistence of planetary mobile robotic exploration: new technology concepts for Mars and beyond. In: Photonics Technologies for Robotics, Automation, and Manufacturing, pp. 43–59. International Society for Optics and Photonics (2003)
[13] Stenning, B., Bajin, L., Robson, C., Peretroukhin, V., Osinski, G.R., Barfoot, T.D.: Towards autonomous mobile robots for the exploration of steep terrain. In: Proceedings of the International Conference on Field and Service Robotics. Springer (2013)
[14] Stroupe, A., Huntsberger, A., Garrett, M., Younse, P.: Robotic Mars Geology with TRESSA: Beyond the Mars Rovers. In: Workshop on Robotics and Challenging Environments, ICRA (2007)
[15] Wettergreen, D., Thorpe, C., Whittaker, R.: Exploring Mount Erebus by walking robot. Robotics and Autonomous Systems **11**(3), 171–185 (1993)